Chemical Engineering Journal 166 (2011) 678–686

Contents lists available at ScienceDirect

Chemical Engineering Journal

journal homepage: www.elsevier.com/locate/cej

Compressibility of biotic sludges – An osmotic approach

Daan Curvers[a,*], Hans Saveyn[a], Peter J. Scales[b], Paul Van der Meeren[a]

[a] Particle and Interfacial Technology Group, Faculty of Bioscience Engineering, Ghent University, Belgium
[b] Particulate Fluids Processing Centre, University of Melbourne, Victoria, Australia

ARTICLE INFO

Article history:
Received 9 June 2010
Received in revised form
11 November 2010
Accepted 11 November 2010

Keywords:
Sludge
Compressibility
Modelling
Osmotic pressure
Donnan equilibrium
Dewatering

ABSTRACT

A simple yet relatively complete model and numerical solution method for describing the effects of osmotic pressure on the compressibility of materials bearing surface charges, and its dependence on bulk solution properties is presented. The basis of this thermodynamic model is Donnan equilibrium and surface charge regulation. The model is capable of explaining effects that were observed in [1] with regard to the effect of salt addition on wastewater treatment sludge compressibility. The simulation results suggest that the filtrate conductivity changes with the level of compression, which was confirmed experimentally. Furthermore, the simulation results suggest a dependence of compressibility on the dewatering method, i.e. on the fate of the expelled water. In case the solution that is expelled from the compressed gel stays in contact with the gel (e.g. centrifugation), the compressibility properties can be different from the properties in case the expelled water is completely removed (e.g. filtration).

1. Introduction

Wastewater sludges, and more generally biotic sludges, are often considered to be hard to dewater. In contrast to most slurries of inorganic nature, they show a non-classic filtration behaviour. It has been observed that during pressure dewatering, an increase in the applied pressure results in only a very weak flux improvement. This has been attributed to the extreme compressibility of biotic sludges, leading to the formation of a highly compressed gel layer, just above the filter medium [2].

Typically in filtration modelling, the compressibility of the solids is expressed using empirically determined constitutive equations. A frequently used equation is the power law function of [3]:

$$\phi = \phi_g \left(1 + \frac{p_s}{p_a}\right)^{\beta}. \quad (1)$$

Many other equations have been suggested for different materials or applications. All of these have been determined empirically and they do not contribute directly to a better understanding of the underlying physical driving forces. The equations do not explain why certain materials behave in a certain way or why exactly a material has a certain functional form describing the relationship between two variables.

Keiding et al. [4,5] introduced the idea that osmotic pressure governs the compressibility behaviour of sludge and – as a consequence – also its filtration behaviour. Earlier, Legrand et al. [6] had pointed out the similarity between wastewater sludge and a low charge anionic gel network with respect to flocculation and deswelling behaviour. This is due to a large fraction of biotic sludges being made up of extracellular polymeric substances (EPS), containing proteins, polysaccharides, humic substances and nucleic acids [7–10], all of which contain charged functional groups. A generally accepted model of sewage sludge consists of aggregated microorganisms embedded in an EPS gel matrix [11–16]. Christensen and Hinge [17] used solid polystyrene cores copolymerised with a charged polyacrylic acid network on the outside as a model system for a microorganism slurry. Seviour et al. [18] made a clear case for understanding the properties of sludge granules – strongly related to sludge flocs – as hydrogels. Curvers et al. [1] showed that the compressibility of wastewater treatment sludge is significantly affected by the bulk salt concentration, indicating a charge related mechanism being at least partly responsible for its compression behaviour. Earlier, Jean and Lee [19] also found a critical salt (NaCl) concentration to increase sludge dewatering efficiency. Higher concentrations were found to reduce the efficiency again, which was attributed to ion exchange leading to floc breakdown.

2. Theoretical background

Keiding and Rasmussen [4] derived a simple equation expressing the osmotic pressure difference as a function of the solids fraction, and state that – together with a Kozeny-Carman type equation for the local cake resistance – this can be used to describe the filtration kinetics for sludge. They start from the Van't Hoff equation

* Corresponding author.
E-mail address: Daan.Curvers@UGent.be (D. Curvers).

1385-8947/$ – see front matter © 2010 Elsevier B.V. All rights reserved.
doi:10.1016/j.cej.2010.11.046

for the osmotic pressure difference $\Delta\Pi$:

$$\Delta\Pi = RT\Delta C, \tag{2}$$

with R the universal gas constant [Pa m^3 K^{-1} mol^{-1}], T the temperature [K] and ΔC the concentration difference [mol/m^3].

Assuming that the total solids stress is equal to the osmotic pressure difference, that the net counterion concentration is equal to the concentration of surface charges, and that dissolved neutral salts do not contribute to a concentration difference between the filter cake and the external bulk, Keiding and Rasmussen [4] transformed Eq. (2) into an expression for the solids pressure p_s:

$$p_s = \Delta\Pi = RT\sigma\rho\frac{(1-\varepsilon)}{\varepsilon}, \tag{3}$$

with σ the charge density [meq/g solid], ρ the solids density [kg/m^3] and ε the porosity of the cake [−].

In this paper, we will look further into the interactions between surface charges and the bulk ion concentration, and the resulting osmotic pressure difference. We will only discuss the part of the osmotic pressure that is due to electrostatic interactions, and try to explain the effects of bulk ionic concentration on sludge compressibility and how this relates to the current usage of compressibility in filtration science. Structural properties (e.g. solid elasticity) as well as other, non-electrostatic effects contributing to the total effective osmotic pressure difference, such as the free energy related to polymer mixing and polymer elasticity [20], are not considered in this model.

A model is developed that is simple enough to allow relatively easy calculation and interpretation. On the other hand, some of the simplifications made in the afforementioned works are dismissed in order to increase the relevance of the model and better explain charge related effects. As a result, the model does not aim to describe the total filtration process nor compressibility to its full extent, but it does offer a way of interpreting the effect of bulk electrolyte concentration on compressibility, and provides a straightforward ability to be used in a more general model, beyond the scope of this paper.

2.1. Osmotic pressure

When two solutions with a different solute concentration are separated by a semipermeable membrane – permeable to the solvent, but impermeable to the solute – solvent will migrate from the compartment with the lowest solute concentration to the one with the highest concentration. This flow can be stopped by applying an extra pressure to the solution with the highest concentration. This is the osmotic pressure difference, often calculated using the Van't Hoff equation [2].

This equation is only valid for dilute ideal solutions. The deviation from ideal behaviour can be expressed by means of an osmotic coefficient $\xi(C)$. The osmotic pressure of a solution with solute concentration C is then given by [21]:

$$\Pi \simeq \xi(C)RTC. \tag{4}$$

The value of the $\xi(C)$ coefficient depends on the solute species and concentration. For different combinations of salts, the osmotic coefficient as a function of the concentration can be found in the literature (e.g. [22,23]). For a solution of NaCl, the osmotic coefficient is given by [22]:

$$\xi = 1 - \frac{S_t\sqrt{d_0}}{A^3 m}\left[(1+A\sqrt{m}) - 2\ln(1+A\sqrt{m}) - \frac{1}{(1+A\sqrt{m})}\right] + Bm + Cm^2 + Dm^3, \tag{5}$$

with m the salt concentration in moles per kg solvent. The variables in Eq. (5) are used for calculating the osmotic coefficient at different temperatures. At 20 °C, $S_t\sqrt{d_0} = 1.1607$, $A = 1.4596$, $B = 1.061\times10^{-2}$, $C = 1.778\times10^{-2}$ and $D = -1.94\times10^{-3}$.

2.2. Charge regulation

Activated sludge surface charges arise from the dissociation of functional groups. Each functional group dissociation is governed by a dissociation constant. Example for a carboxyl group:

$$K_a = \frac{[\mathrm{COO^-}]\cdot[\mathrm{H^+}]}{[\mathrm{COOH}]}. \tag{6}$$

It is clear from Eq. (6) that the degree of dissociation depends on the pH within the gel but also plays a role in determining it. Even though the effect of charge regulation can be significant, it is often omitted in the modelling of polyelectrolyte swelling pressure [4,24,25]. This leads to an overestimation of the surface charge density in most cases except when the charged groups are in the salt form, i.e. each surface charge is compensated by a dissociated counterion and the hydronium concentration is low in comparison to the counterion concentration. Other models calculate the dissociation degree based on the bulk pH [26]. This yields a more versatile model, but still imposes some restrictions as a fixed bulk pH has to be known or assumed. For the model presented herein, charge regulation is included by assuming a pK_a value for the surface charges and including Eq. (6) in the overall mass balance. This leads to a dissociation number α, indicating the fraction of ionisable functional groups that are effectively dissociated:

$$K_a = \frac{\alpha fc_p\cdot[\mathrm{H^+}]}{(1-\alpha)fc_p} = \frac{\alpha\cdot[\mathrm{H^+}]}{(1-\alpha)}, \tag{7}$$

with fc_p the total concentration of available ionisable groups ($fc_p = [\mathrm{COO^-}] + [\mathrm{COOH}]$). Only one p$K_a$ value was chosen for simplicity's sake, but the mass balance can be supplemented with additional pK_a values. Dignac et al. [27] found glutamic acid (side chain pK_a 4.07) and aspartic acid (pK_a 3.86) to be the most abundant amino acids in activated sludge EPS. As such, calculations will be based on a pK_a value of 4.00. The dissociation constant for Na^+ is much higher than the dissociation constant for hydroxonium [28], and counterion condensation (Manning condensation) is not normal for weakly charged gels, such as EPS. At high Na^+ concentrations, counterion condensation can take place, but this effect has not been considered hereafter.

3. The model system

3.1. Assumptions

A gel system, consisting of a weakly charged cross-linked polyanion gel with its counterions (Na^+), dissolved in a solvent (water) and surrounded by a bulk with a certain concentration of a neutral salt (NaCl) is considered. It is assumed that all changes within the gel are isotropic, so for a given applied pressure, the average solids concentration is constant throughout the gel. The gel is in equilibrium with an external bulk solution. Of interest is the pressure p_s that is required to increase the polymer concentration in the gel to a certain level and the effect of the bulk ion concentration on this pressure.

A second assumption has to be made with regard to the bulk solution. This solution can be regarded either as an infinite reservoir with a constant salt concentration, as an initial volume of solvent with an initial salt concentration, or it can be assumed to be non-existent. None of these situations apply to reality, but it can be expected that in the case of equilibrium centrifugation, the second situation will be the best approximation. When starting with a reasonably dilute suspension, the first case and the second situation

will yield comparable results. Pressure filtration, on the other hand, is probably more closely resembled by the third, as in most cases, the water expelled from the gel is physically separated from the gel. The first situation is both more trivial to calculate and less relevant to actual dewatering processes than the other two cases, so it will not treated in this instance.

3.2. Governing equations

3.2.1. Constant total volume

The *first case* considered is a system with a constant total solution volume V_{tot}. Water expelled from the gel – upon increase of the solids pressure p_s – is added to the bulk, and contributes to the bulk ion concentrations. As follows from above, the thermodynamic equilibrium is governed by the following set of equations:

$$V_{in} \cdot [Na^+_{in}] + V_{out} \cdot [Na^+_{out}] = [Na^+_{tot}] \cdot V_{tot}; \quad (8)$$

$$V_{in} \cdot [Cl^-_{in}] + V_{out} \cdot [Cl^-_{out}] = [Cl^-_{tot}] \cdot V_{tot}; \quad (9)$$

$$[H_3O^+_{in}] \cdot [OH^-_{in}] = 10^{-14}; \quad (10)$$

$$[H_3O^+_{out}] \cdot [OH^-_{out}] = 10^{-14}; \quad (11)$$

$$[H_3O^+_{in}] + [Na^+_{in}] = \alpha \cdot fc_p + [OH^-_{in}] + [Cl^-_{in}]; \quad (12)$$

$$[H_3O^+_{out}] + [Na^+_{out}] = [OH^-_{out}] + [Cl^-_{out}]; \quad (13)$$

$$[Na^+_{in}] \cdot [Cl^-_{in}] = [Na^+_{out}] \cdot [Cl^-_{out}]; \quad (14)$$

$$K_a = \frac{\alpha \cdot [H^+]}{(1-\alpha)}; \quad (15)$$

$$\frac{[Na^+_{in}]}{[Na^+_{out}]} = \frac{[H_3O^+_{in}]}{[H_3O^+_{out}]}. \quad (16)$$

The square brackets designate concentrations, the subscripts indicate the position: the bulk solution (out), the solution within the gel (in) or the sum of both (tot). In Eqs. (10), (11), (14)–(16), concentrations are used as an approximation of the corresponding activities. (Note that upon solving these equations, a better approximation of the activities can always be found using the calculated concentrations for determining the ionic strength.) Eqs. (8) and (9) express the conservation of Na^+ and Cl^- ions within the system. Eqs. (10) and (11) denote the dissociation equilibrium of water. Eqs. (12) and (13) express electroneutrality in both compartments. Eq. (14) expresses that the total activity of the neutral salt is equal in both compartments, Eq. (15) is equal to Eq. (7) and Eq. (16) refers to the fact that the ratio of the concentrations in both compartments is equal for equally charged ions, as dictated by the electrochemical potential.

Note that Eqs. (8), (9) and (12) allow to specify whether the polyanion is added to the system in the salt form (Na^+ as counterion), or as an acid (initially not dissociated). For the case where all groups are initially present in the acid form, $[Na^+_{tot}] \cdot V_{tot} = [Cl^-_{tot}] \cdot V_{tot}$; when all groups are present in the salt form, $[Na^+_{tot}] \cdot V_{tot} = [Cl^-_{tot}] \cdot V_{tot} + fc_p \cdot V_{in}$. A combination of the salt and the acid forms results in a Na^+ concentration between these extremes. Concentrations outside this range correspond to the addition of either NaOH or HCl and will influence the bulk pH.

This set of equations cannot be solved analytically in a trivial way, but it can be simplified into a set of two equations in two unknowns, which can then be solved numerically. More information about the numerical solving method can be found in Appendix A.

3.2.2. Removal of expelled solution

The *second scenario* considered is a system where the solution that is expelled from the gel is physically removed from the system. As a result, the equilibrium is no longer influenced by a surrounding bulk solution. Simulating this effect is done by starting with a gel that fills the total system (no free bulk present), and considering a very small increase in ϕ. This increase in ϕ corresponds with a small volume of solution that is expelled from the gel. For this situation, the system of equations (8)–(16) is solved with V_{out} being the small volume of solution that has been expelled from the gel. Then, this volume is subtracted from the total system, and the total Na^+ and Cl^- concentrations are changed accordingly. Note that this is a radical simplification of the filtration process, as in reality, filtration is not an isotropic process, i.e. a range of different volume fractions and solids pressures are present within the filter cake during filtration.

The total amount of Na^+ and Cl^- within the system no longer remains constant. Once these ions are removed, they can no longer influence the gel equilibrium. As such, it can be expected that the osmotic pressure difference (between the gel and the water that has been expelled but not yet removed) as a function of the solids volume fraction is different from the former case.

In both cases, the net osmotic pressure can be calculated as the difference between the osmotic pressure within the gel and in the bulk, according to Eq. (4).

4. Materials and methods

4.1. Crosslinked polyacrylic acid

Filtration experiments were performed on a commercially available cross-linked polyacrylic acid gel ('poly(acrylic acid), partial sodium salt-graft-poly(ethylene oxide), cross linked', Aldrich Chemistry, Germany). Gel suspensions (4 g/L) were prepared in demineralised water with a background conductivity of 5 μS/cm. The suspensions were prepared and stirred for at least 24 h prior to the dewatering experiments to ensure complete hydration.

4.2. Filtrate conductivity

Filtrations were performed on a lab-scale dead-end filtration setup, described in more detail in [29]. The displacement of the piston was used to monitor the filtrate volume. The filtrations were performed on a volume of 250 mL of suspension at two different pressures (300 and 500 kPa). The filtrate outlet of the filtration rig was directly connected to the measuring cell of a conductivity meter (Consort K612 with Consort SK10T electrode). To guide the liquid through the electrode and to restrict the measuring volume, the electrode was closed off using flexible tubing. As the electrode cell is designed to be totally immersed in the liquid, this restriction makes that the results cannot be interpreted as absolute conductivity figures, but have to be considered in a relative way. To reduce evaporation effects, the exit for the liquid was restricted to a small hole. It was checked that the liquid velocity did not have a significant influence on the conductivity measurement.

5. Results

5.1. Case 1: constant total volume

All calculations were performed using a pK_a value of 4, and a total available surface charge density of −0.5 meq/g suspended solids [30]. To transform this surface charge density into a volumetric surface charge concentration, a density of 1500 kg/m^3 was assumed. The temperature was set at 20 and the calculations were performed with a 450 bit precision (cf. Appendix A).

Fig. 1 demonstrates the importance of including charge equilibria and the initial state of the functional groups in the model. In the legend, f(Na) denotes the fraction of all available ionisable groups

Table 1
Calculated concentrations and derived variables for a gel with a pK_a value of 4.00, a surface charge density of −0.5 meq/g, an initial solids volume fraction of 0.01 and a bulk solution of 0.25 M NaCl at a solids volume fraction ϕ of 0.05 and 0.30 and with f(Na) = 0.0, 0.5 and 1.0.

f(Na)	ϕ = 0.05			ϕ = 0.30		
	1.0	0.5	0.0	1.0	0.5	0.0
$\Delta\Pi$ [kPa]	3.452	0.913	0.041	211.325	58.479	2.564
α	0.9999	0.5122	0.1081	0.9998	0.5093	0.1052
Cl^-_{in} [M]	0.235	0.242	0.248	0.139	0.183	0.234
Cl^-_{out} [M]	0.254	0.252	0.250	0.253	0.252	0.250
Na^+_{in} [M]	0.274	0.262	0.252	0.460	0.346	0.267
Na^+_{out} [M]	0.254	0.252	0.250	0.253	0.252	0.250
pH_{in}	7.929	4.021	3.084	7.813	4.016	3.070
pH_{out}	7.962	4.039	3.087	8.074	4.155	3.099

that are initially in the salt form (as shown in Section 3.2.1, determined by Eqs. (8), (9) and (12)). For f(Na) = 1, all groups are initially in the salt form (and ionised). For f(Na) = 0, all groups are added in the acid form and *can* be ionised, as determined by the dissociation constant. The bulk salt concentration was set at 0.25 M, the ratio of the volume of solids in the gel to the total volume (gel + bulk) was 0.01. Some extra simulation results are shown in Table 1. At a solids volume fraction in the gel of 0.30, the osmotic pressure differences are 211.3, 58.5 and 2.6 kPa respectively for f(Na) = 1, 0.5 and 0. The large differences between these osmotic pressures are due to the fact that, in case of the acid form, most of the functional groups are actually not dissociated. For lower pK_a values (stronger acids), the dissociated fraction will be higher. In this case, at a solids volume fraction of 0.30, and for a pK_a value of 4, the fraction of dissociated functional groups is 0.9998, 0.5093 and 0.1052 respectively for f(Na) = 1, 0.5 and 0, as shown in Table 1. This means that the number of available charges for f(Na) = 0 is only ≈10% of the number of charges for f(Na) = 1.

As discussed by Mikkelsen [30], it is hard to discern between ionised and ionisable functional groups, and different measuring methods can yield different results. It is unconceivable, however, that either all functional groups are in salt form or all are in acid form. For further calculations, a f(Na) = 0.5 will be used.

Fig. 2 shows the effect of bulk electrolyte concentration on the osmotic pressure difference between the gel and the bulk. Clearly, increasing the electrolyte concentration leads to a decrease of the osmotic pressure difference. Accordingly, for a given pressure, a higher solid content will be reached upon increasing the bulk electrolyte concentration. At a solids pressure of 100 kPa, for example, solids volume fractions of 0.27, 0.36 and 0.43 will be reached with this system for bulk electrolyte concentrations of 0.10, 0.25 and 0.50 M respectively. This agrees with the experimental data from [1], where addition of NaCl led to an increase of the solids volume fraction, both in filtration and centrifugation experiments. Table 2 gives an overview of the osmotic pressure differences at a solids volume fraction of 0.30 for different bulk salt concentrations, as well as calculated concentrations and derived variables. An interesting effect is that of salt addition on the bulk pH. In the absence

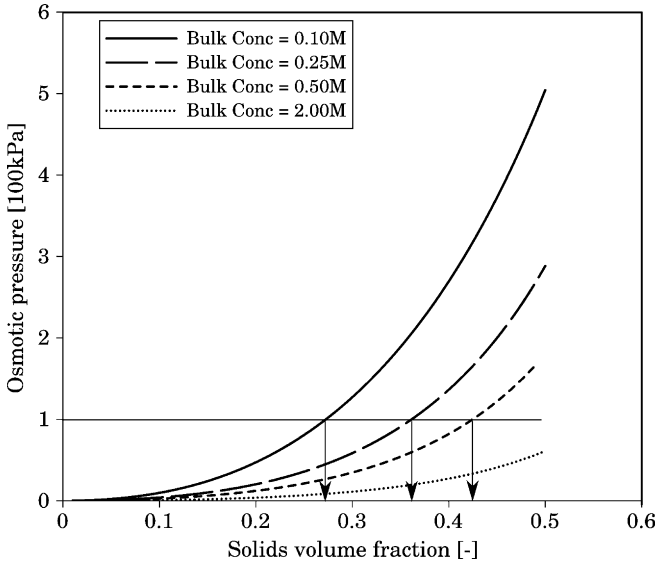

Fig. 2. The effect of bulk electrolyte concentration on the overall osmotic pressure difference for a gel with a pK_a value of 4.00, a surface charge density of −0.5 meq/g, an initial solids volume fraction of 0.01 and an initial fraction in the salt form f(Na) of 0.5.

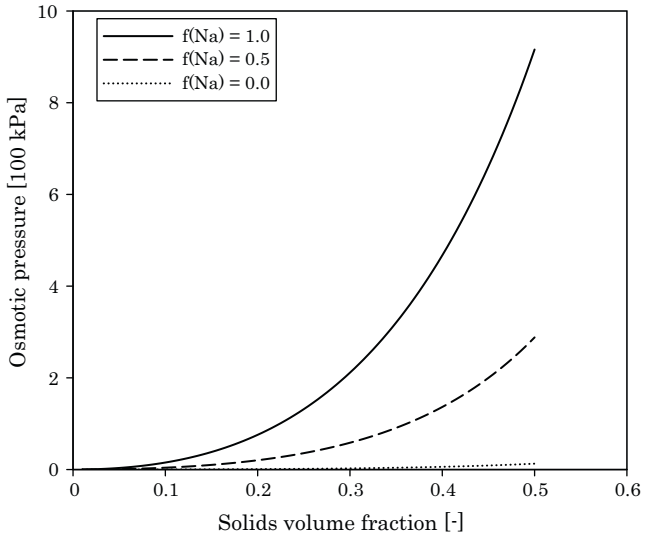

Fig. 1. The effect of charge equilibria and the initial state of the functional groups on the total osmotic pressure difference for a gel with a pK_a value of 4.00, a surface charge density of −0.5 meq/g, an initial solids volume fraction of 0.01 and a bulk solution of 0.25 M NaCl. f(Na) denotes the fraction of all available ionisable groups that are added to the system in the salt form.

Table 2
The osmotic pressure difference at a solids volume fraction of 0.30 for a gel with a pK_a value of 4.00, a surface charge density of −0.5 meq/g, an initial solids volume fraction of 0.01 and an initial fraction in the salt form f(Na) of 0.5 at different bulk electrolyte concentrations.

Bulk conc. [M]	0.01	0.10	0.25	0.50
$\Delta\Pi$ [kPa]	318.32	127.21	58.48	31.59
α	0.501	0.506	0.509	0.511
Cl^-_{in} [M]	0.001	0.049	0.183	0.426
Cl^-_{out} [M]	0.010	0.101	0.252	0.502
Na^+_{in} [M]	0.162	0.211	0.346	0.590
Na^+_{out} [M]	0.010	0.101	0.252	0.502
pH_{in}	4.002	4.011	4.016	4.019
pH_{out}	5.201	4.330	4.155	4.089

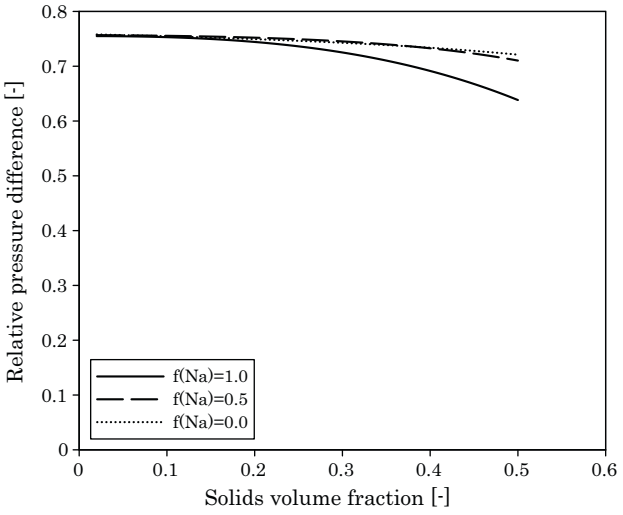

Fig. 3. The relative decrease in solid pressure required for reaching a given solids volume fraction with a bulk electrolyte concentration of 0.20 M and 1.00 M NaCl respectively as a function of the solids volume fraction for different forms of the ionisable groups in a system where the expelled water remains in contact with the gel.

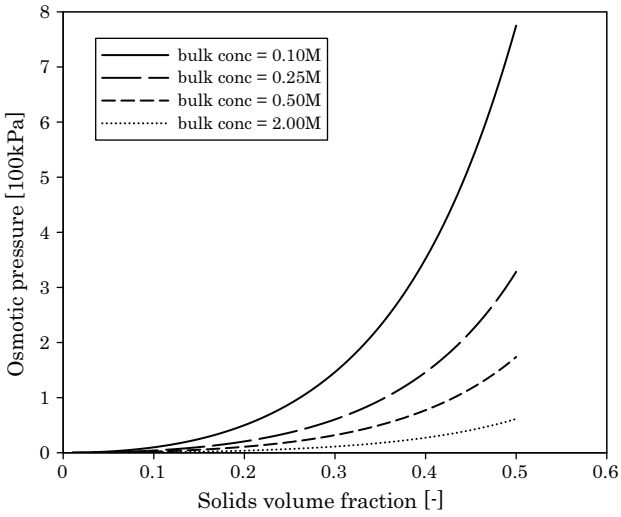

Fig. 4. The effect of bulk concentration on the overall osmotic pressure difference. Increasing the bulk pressure reduces the total osmotic pressure difference.

of electrolyte, the dissociated protons are kept within the gel for reasons of electroneutrality, whereas when Na^+-ions are present in the bulk, these can exchange with the protons in the gel, leading to an increased pH inside the gel, and a decreased pH in the free bulk. Note that the pH values in Table 2 are derived from the calculated proton concentration whereas in reality, the pH is based on the proton activity. The activity coefficient is lower for higher electrolyte concentration (higher ionic strength), which results in higher pH values in reality. This is to some extent compensated for by the fact that the dissociation is also based on activity, which would, in reality, lead to a higher degree of dissociation as well.

Fig. 3 shows the relative decrease in solids pressure required to reach a given solids volume fraction with a bulk electrolyte concentration of 0.20 M and 1.00 M NaCl respectively $([\Delta\Pi_{0.2\,M} - \Delta\Pi_{1\,M}]/\Delta\Pi_{0.2\,M})$ as a function of said solids volume fraction for different forms of the ionisable groups (salt or acid form). It illustrates the relative effect of adding salt on the osmotic pressure difference. For the simulated system, the increase of the bulk electrolyte brings about a decrease of the required pressure to reach a given solids volume fraction of around 75%. At increasing solids pressures, or increasing solids volume fractions, the relative effect of adding salt on the overall osmotic pressure difference lessens. This seems in contrast with what was observed for equilibrium centrifugation by Curvers et al. [1]. In this study, an increase in the relative effect was observed for centrifugation. At the lower pressures, however, which are relevant to sludge centrifugation, the decrease in the relative effect of salt addition is very small.

Interestingly, the effect of salt addition is higher when all functional groups are in the acid form than when they are in the salt form. This is due to the fact that in this case, less functional groups are ionised, and the relative abundance of $[Na^+_{in}]$ over the surface charges is higher. As shown above, the number of available charges for $f(Na) = 0$ is only ≈10% of the number of charges for $f(Na) = 1$. Hence, the relative excess of NaCl is 10 times as large, making the effect of adding (a fixed amount of) salt stronger.

5.2. Case 2: filtrate removal

Fig. 4 shows the effect of bulk concentration on the osmotic pressure difference between the gel and the bulk. When comparing this to Fig. 2, it is clear that both cases result in different osmotic pressure differences, and as such, different material behaviours. In the second case, a higher solid pressure is required to reach a given solids volume fraction. The difference can also be observed in Fig. 3 in comparison to Fig. 5, where the former shows distinctly more dependence on the solids volume fraction. This means that for materials where compressibility is largely determined by osmotic pressure (charged systems at relatively low salt concentrations), their behaviour during dewatering can be different for different dewatering methods.

Fig. 6 shows the influence of compression on the pH and Na^+ concentration of the solution expelled from a gel with a pK_a value of 4.00, a surface charge density of −0.5 meq/g, an initial solids volume fraction of 0.01, an initial electrolyte concentration of 0.1 M and $f(Na)$ set to 0.5. The pH calculation is based on the simulated $[H_3O^+_{out}]$ concentrations. The salt concentration in the expelled solution decreases with increasing levels of compression. This is due to the Donnan equilibrium, implying a higher neutral salt concentration outside the gel, leading to a depletion of the salt levels within the gel.

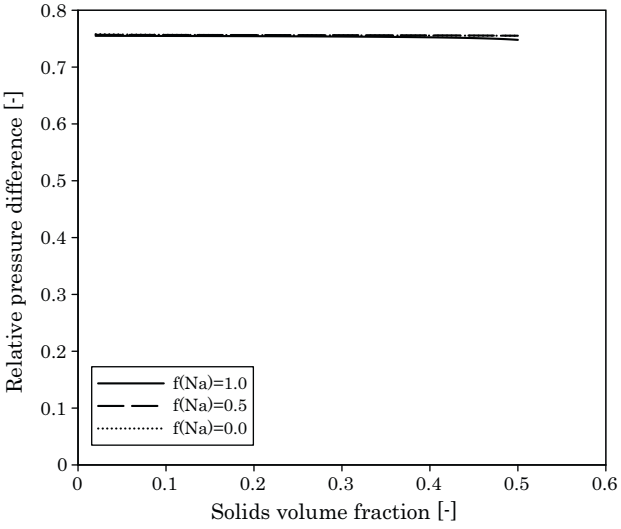

Fig. 5. The relative decrease in solid pressure required for reaching a given solids volume fraction with a bulk electrolyte concentration of 0.20 M and 1.00 M NaCl respectively as a function of the solids volume fraction for different forms of the ionisable groups in a system where the expelled water is removed.

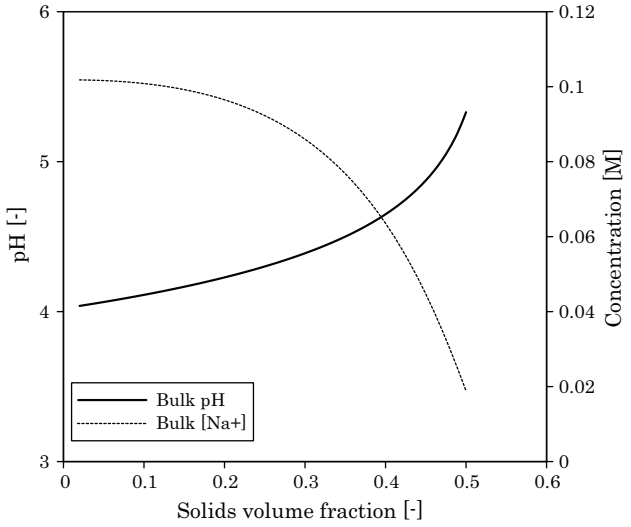

Fig. 6. The pH and the Na^+ concentration in the bulk (expelled from the gel) as a function of the solids volume fraction for a gel with a pK_a value of 4.00, a surface charge density of −0.5 meq/g, an initial solids volume fraction of 0.01 and an initial electrolyte concentration of 0.1 M.

5.3. Filtrate conductivity

Fig. 6 also shows that the salt concentration in the solution expelled from the gel decreases with an increasing level of compression. On the basis of this information, one expects the conductivity of filtrate of a polyelectrolyte gel to decrease as filtration proceeds. It has to be stressed once more, that the overall filtration process is much more complex than the system presented in case 2, as, for compressible materials, different levels of compression are attained at different positions within the filter cake at any given time. Fig. 7 shows the filtrate conductivity as a function of time for two filtration experiments with 250 mL of a cross-linked polyacrylic acid gel supension. Together with the conductivity, the figure also shows the squared filtrate volume (expressed as squared piston displacement) as a function of time. Fig. 7 clearly shows the conductivity to be decreasing over time during filtration, which is an indication of a decreasing free ion concentration. This is in accordance with what one would expect based on the simulation results. Interestingly, the conductivity starts rising again at the end of the filtration (marked by the end of the semi-linear region in the squared filtrate volume vs. time). There are several possible explanations for this observation. First, liquid from higher regions in the filter cake, being expelled from the gel in an earlier stage and at lower solids pressures, can be pushed through the filter cake and result in an increased filtrate conductivity. Secondly, the sharp decrease in liquid flow that accompanies the transition to the expression phase can be expected to increase the relative importance of evaporation. Finally, at very low liquid velocities, diffusion might start to play a significant role as well, leading to new equilibria. It is to be expected that this particular effect is due to a combination of all of the aforementioned phenomena, possibly together with other, less conspicuous effects.

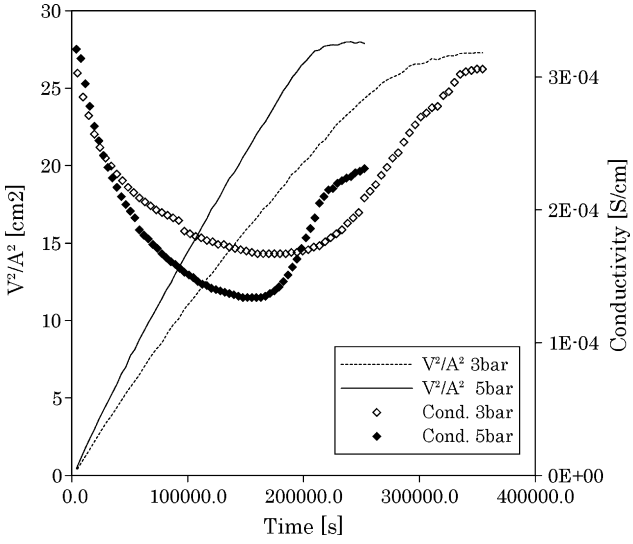

Fig. 7. The filtrate conductivity and squared piston displacement as a function of time for dead-end filtration of 4 g/L cross-linked polyacryic acid gels at 300 and 500 kPa.

6. Discussion

The filtration of compressible materials is a complex process, which can be simulated relatively accurately based on empirically determined relationships between local solids pressure, local solids volume fraction and local filtration resistance [2,31]. Not much is known, however, about the basic principles that govern these empirical relationships. For a complex material, like a biotic sludge, the total compressibility behaviour will be governed by a range of different factors. From the above, it is clear that osmotic phenomena can play an important role in determining the dewaterability properties of some materials. The importance of osmotic pressure over structural properties (e.g. material elasticity) in turn depends on both material properties like the abundancy of ionisable groups and their pK_a values, and on bulk properties like salt concentrations and pH. Curvers et al. [1] showed that for a biotic wastewater sludge, the osmotic pressure difference does make up a considerable fraction of the total resistance against compression. The results above show that theoretically, with parameters chosen carefully to reflect as good as possible the sludge EPS gel matrix, this is to be expected as well. While the simulation results yield realistic pressure values, some important parameters are still not sufficiently known. As pointed out by Mikkelsen [30], it is hard to discern between ionised and ionisable functional groups. This information is required, however, for creating a reliable model for surface charge effects. If the status of the functional groups can be determined accurately, this model can be a step towards predicting (biotic) sludge compressibility based on fundamental physico-chemical properties.

In Curvers et al. [1], somewhat different behaviours were observed for centrifugation and filtration compressibility. In the case of centrifugation, the relative pressure difference upon addition of salt was observed to increase with increasing pressure, while for filtration the opposite was observed. This was attributed to fitting errors and measurement errors, as well as to the difference in the pressure range (0–2000 Pa for centrifugation vs. 50–2000 kPa for filtration). The model indicates that it is theoretically possible for a given material bearing surface charges to show a compressibility behaviour in gravity settling and centrifugation that is different from the behaviour observed during filtration. In the first case, the expelled solution remains in contact with the gel, and can still have an influence on the equilibrium concentrations. In the second case, the expelled solution is completely removed, and can no longer influence the equilibrium between gel and bulk. It has to be mentioned that both simulated cases are idealisations of the centrifugation and filtration process and are unlikely to fully represent their real world counterparts, and that only electrostatic interactions are considered here. The simulations confirm the observed effects insofar that in both cases, the decrease in relative pressure difference as a function of solids volume fraction is more distinct at higher solids volume fractions. It cannot be ascertained from

this to what extent the effect plays an important role in the compressibility of wastewater sludges, but it does offer a supplemental explanation for the experimentally observed differences between centrifugation and filtration.

It is clear that charge equilibria and the state of the (charge bearing) functional groups are important factors in determining the compressibility behaviour of materials containing surface charges. In sewage sludges, the effect of charge regulation might be diminished by the presence of pH buffering agents. On the other hand, the charge regulation mechanism itself acts as a buffer system as well, and makes up at least a part of the sludge's total buffer capacity.

An interesting effect, seen both in simulations and in experimental data, is the change of the filtrate composition with the level of compression. Starting from a homogeneous polyelectrolyte gel suspension, the measured filtrate conductivity decreases over time during the filtration phase. This agrees with the simulation results which indicate that the ion concentration decreases upon further compression and serves as an extra indication that charge related processes take place during filtration and compression, and play a role in determining the material behaviour.

The model system used here, based on polyacrylic acid, is – on purpose – not nearly as complex as biotic sludge systems and can only represent – to some extent – the EPS fraction of activated sludge. Results from physico-chemical analyses found in the literature do suggest, however, that EPS makes up a large fraction of the total sludge biomass and acts as a weakly charged polymer networks. There's also experimental evidence that charge effects play a prominent role in the overall compressibility of biotic sludges [1,19]. With this in mind, the above compressibility model can serve to explain the major phenomena that are observed in relation to charge effects. It is clear that these effects will be negligible in systems where the compressibility behaviour is determined by non charge related effects, e.g. coagulated inorganic particles, where compressibility can be defined in terms of a yield stress, leading to irreversible restructing of the solids. On the other hand, the osmotic pressure can be expected to play a role in dewatering of, for instance, stable colloidal systems, where the importance of the surface charges shows already in their stabilising role.

7. Conclusions

A simple yet relatively complete model and numerical solution method for describing the effects of osmotic pressure on the compressibility of materials bearing surface charges, and its dependence on bulk solution properties is presented. Even though the model is not a complete model for total compressibility (lacking structural components), it is capable of explaining the effects that were observed in [1] with regard to the effect of salt addition on sewage sludge compressibility.

Besides stressing the importance of proper surface charge determination, the simulation results also suggest a dependence of compressibility on the dewatering method. In the case where the solution that is removed from the compressed gel stays in contact with the gel (e.g. typical centrifugation), the compressibility properties can be different from the properties in case the expelled water is completely removed (e.g. filtration).

Acknowledgements

Daan Curvers acknowledges thankfully the support he receives from Research Foundation – Flanders (FWO) as an aspirant of the foundation. Furthermore, support for this work from the Particulate Fluids Processing Centre, A Special Research Centre of the Australian Research Council, is gratefully acknowledged.

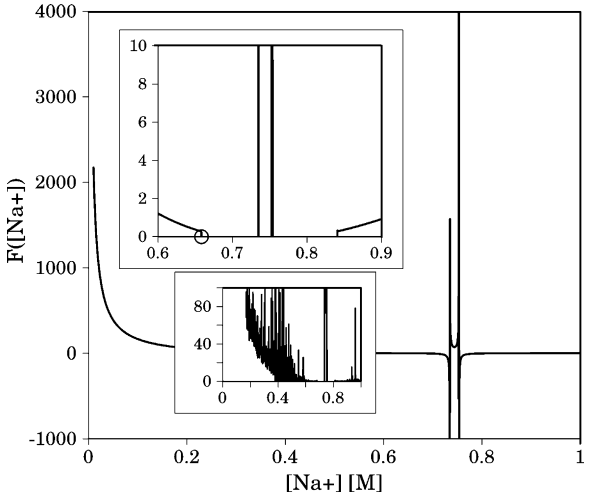

Fig. 8. The typical form of $F([Na^+_{in}])$, showing the difficulties encountered when seeking its solutions. The largest inset shows a close-up of the region of interest, with the circle indicating the physically meaningful solution. The small inset shows $F([Na^+_{in}])$ calculated with 53 bit precision.

Appendix A. Numerical solution method

Eqs. (8)–(11) and Eqs. (14)–(16) can be converted into:

$$[H_3O^+_{out}] = \frac{[Na^+_{tot}]\cdot V_{tot}\cdot[H_3O^+_{in}] - [Na^+_{in}]\cdot V_{in}\cdot[H_3O^+_{in}]}{[Na^+_{in}]\cdot V_{out}}; \tag{A.1}$$

$$[OH^-_{out}] = \frac{10^{-14}\cdot[Na^+_{in}]\cdot V_{out}}{[Na^+_{tot}]\cdot V_{tot}\cdot[H_3O^+_{in}] - [Na^+_{in}]\cdot V_{in}\cdot[H_3O^+_{in}]}; \tag{A.2}$$

$$[OH^-_{in}] = \frac{10^{-14}}{[H_3O^+_{in}]}; \tag{A.3}$$

$$[Na^+_{out}] = \frac{[Na^+_{tot}]\cdot V_{tot} - [Na^+_{in}]\cdot V_{in}}{V_{out}}; \tag{A.4}$$

$$[Cl^-_{out}] = \frac{[Cl^-_{tot}]\cdot V_{tot}\cdot[Na^+_{in}]\cdot V_{out}}{[Na^+_{in}]\cdot V^2_{out} + [Na^+_{tot}]\cdot V_{tot}\cdot V_{in} - [Na^+_{in}]\cdot V^2_{in}}; \tag{A.5}$$

$$[Cl^-_{in}] = \frac{[Cl^-_{tot}]\cdot V_{tot}\cdot[Na^+_{in}]\cdot V_{in} - [Cl^-_{tot}]\cdot[Na^+_{tot}]\cdot {V_{tot}}^2}{[Na^+_{in}]\cdot {V_{in}}^2 - [Na^+_{in}]\cdot {V_{out}}^2 - [Na^+_{tot}]\cdot V_{tot}\cdot V_{in}}; \tag{A.6}$$

$$\alpha = \frac{K_a}{[H_3O^+_{in}] + K_a}. \tag{A.7}$$

These can then be subsituted into Eqs. (12) and (13) to yield:

$$[H_3O^+_{in}] + [Na^+_{in}] = \frac{K_a}{[H_3O^+_{in}] + K_a}\cdot fc_p + \frac{10^{-14}}{[H_3O^+_{in}]} + \frac{[Na^+_{tot}]\cdot[Cl^-_{tot}]\cdot V^2_{tot} - [Cl^-_{tot}]\cdot V_{tot}\cdot V_{in}\cdot[Na^+_{in}]}{[Na^+_{in}]\cdot V^2_{out} + [Na^+_{tot}]\cdot V_{tot}\cdot V_{in} - {V_{in}}^2\cdot[Na^+_{in}]}; \tag{A.8}$$

$$\frac{[H_3O^+_{in}]\cdot([Na^+_{tot}]\cdot V_{tot} - [Na^+_{in}]\cdot V_{in})}{[Na^+_{in}]\cdot V_{out}} + \frac{[Na^+_{tot}]\cdot V_{tot} - [Na^+_{in}]\cdot V_{in}}{V_{out}} = \frac{10^{-14}\cdot[Na^+_{in}]\cdot V_{out}}{[Na^+_{tot}]\cdot V_{tot}\cdot[H_3O^+_{in}] - [H_3O^+_{in}]\cdot[Na^+_{in}]\cdot V_{in}} + \frac{[Cl^-_{tot}]\cdot V_{tot}\cdot[Na^+_{in}]\cdot V_{out}}{[Na^+_{in}]\cdot V^2_{out} + [Na^+_{tot}]\cdot V_{tot}\cdot V_{in} - [Na^+_{in}]\cdot V^2_{in}}. \tag{A.9}$$

Eq. (A.9) is a second order equation in $[H_3O^+_{in}]$, which can be solved for $[H_3O^+_{in}]$. This yields two roots, one of which is negative. The positive root is:

$$[H_3O^+_{in}] = -\frac{1}{2}\cdot\Big([Na^+_{in}]^3\cdot V_{in}^3 - 2\cdot[Na^+_{tot}]\cdot V_{tot}\cdot[Na^+_{in}]^2\cdot V_{in}^2 + [Na^+_{tot}]\cdot V_{tot}^2\cdot[Na^+_{in}]\cdot V_{in} - ([Na^+_{in}]^3\cdot V_{in} + ([Cl^-_{tot}]-[Na^+_{tot}])\cdot V_{tot}\cdot[Na^+_{in}]^2)\cdot V_{out}{}^2 - ([Na^+_{in}]^4\cdot V_{in}^6 - 4\cdot[Na^+_{tot}]\cdot V_{tot}\cdot[Na^+_{in}]^3\cdot V_{in}^5 + 6\cdot[Na^+_{tot}]\cdot V_{tot}^2\cdot[Na^+_{in}]^2\cdot V_{in}^2 - 4\cdot[Na^+_{tot}]\cdot V_{tot}^3\cdot[Na^+_{in}]\cdot V_{in}^3 + [Na^+_{tot}]\cdot V_{tot}^4\cdot V_{in}^2 + ([Na^+_{in}]^4\cdot V_{in}^2 + 2\cdot([Cl^-_{tot}]\cdot V_{tot} - [Na^+_{tot}]\cdot V_{tot})\cdot[Na^+_{in}]^3\cdot V_{in} + ([Cl^-_{tot}]\cdot V_{tot}^2 - 2\cdot[Cl^-_{tot}]\cdot V_{tot}\cdot[Na^+_{tot}]\cdot V_{tot} + [Na^+_{tot}]\cdot V_{tot}^2)\cdot[Na^+_{in}]^2)\cdot V_{out}^4 - 2\cdot([Na^+_{in}]^4\cdot V_{in}^4 + ([Cl^-_{tot}]\cdot V_{tot} - 3\cdot[Na^+_{tot}]\cdot V_{tot})\cdot[Na^+_{in}]^3\cdot V_{in}^3 - (2\cdot[Cl^-_{tot}]\cdot V_{tot}\cdot[Na^+_{tot}]\cdot V_{tot} - 3\cdot[Na^+_{tot}]\cdot V_{tot}^2)\cdot[Na^+_{in}]^2\cdot V_{in}^2 + ([Cl^-_{tot}]\cdot V_{tot}\cdot[Na^+_{tot}]\cdot V_{tot}^2 - [Na^+_{tot}]\cdot V_{tot}^3)\cdot[Na^+_{in}]\cdot V_{in})\cdot V_{out}^2 + 4\cdot([Na^+_{in}]^2\cdot V_{out}^6 - 2\cdot([Na^+_{in}]^2\cdot V_{in}^2 - [Na^+_{tot}]\cdot V_{tot}\cdot[Na^+_{in}]\cdot V_{in})\cdot V_{out}^4 + ([Na^+_{in}]^2\cdot V_{in}^4 - 2\cdot[Na^+_{tot}]\cdot V_{tot}\cdot[Na^+_{in}]\cdot V_{in}^3 + [Na^+_{tot}]\cdot V_{tot}^2\cdot V_{in}^2)\cdot V_{out}^2)\cdot 10^{-14})^{-1/2}\cdot[Na^+_{in}]]\cdot[[Na^+_{in}]^2\cdot V_{in}^3 - 2\cdot[Na^+_{tot}]\cdot V_{tot}\cdot[Na^+_{in}]\cdot V_{in}^2 - ([Na^+_{in}]^2\cdot V_{in} - [Na^+_{tot}]\cdot V_{tot}\cdot[Na^+_{in}])\cdot V_{out}^2 + [Na^+_{tot}]\cdot V_{tot}^2\cdot V_{in}]^{-1}. \tag{A.10}$$

Substituting Eq. (26) into (24) and grouping all terms on one side yields an equation with one unkown: $F([Na^+_{in}]) = 0$. Once the solution $[Na^+_{in}]$ is determined, the other variables can be calculated using the equations mentioned above. $F([Na^+_{in}])$ cannot be solved analytically, however, and its root has to be found numerically. Fig. 8 shows the typical form of $F([Na^+_{in}])$, and its peculiarities that can hamper finding the solution. The circle marks the only solution that yields physically realistic (i.e. positive) values for the other concentrations. The function is not smooth near the solution and shows a very steep slope at the solution value, which renders root-finding algorithms based on derivation nearly useless (e.g. Newton's method or its more efficient derivatives). Furthermore, between the two extreme zeros the function goes to infinite values. Finally, for higher levels of compression, the two extreme solutions approach each other and the function itself gets steeper at the solution.

A method that proved satisfying under most conditions is as follows. At low levels of compression, the extreme solutions are far apart, and a differentiation based method can be used to find an interval comprising the solution (i.e. positive function value on the left side and negative on the right). Once such an interval has been found, the bisection method is used to find the solution. When the solution has been found for a first series of solid volume fractions (e.g. the first five values), a Lagrange extrapolation of the last solutions is used to make an estimate of each new solution (at a higher solids volume fraction). Then, a small region around the estimate is searched for an interval comprising the solution, upon which the bisection method can be used again. A final hindrance is that $F([Na^+_{in}])$ cannot be calculated using double precision floating point variables. With a precision of 53 bits (IEEE 754 double precision binary floating-point format), rounding errors make the calculation of $F([Na^+_{in}])$ erroneous, as shown in the smallest inset of Fig. 8. This renders any root finding algorithm ineffective. Therefore, all calculations were performed with a precision of 450 bits, using the open source mathematical package Sage [32].

A.1. Result checking

Due to the difficulties associated with finding the correct solution for $F([Na^+_{in}])$, different levels of result checking were implemented. The first, and most simple method of checking the validity of the results is looking at their physical relevance. When an incorrect root is chosen for either Eq. (24) or (26), calculating the other variables will result in negative concentrations. Secondly, after calculating all concentrations, the results were subsituted into Eqs. (8)–(16). Theoretically, upon grouping all terms on one side, these equations have to return zero upon subsitution of the correct solutions. Therefore, the maximum deviation was checked at the end of the algorithm. At a precision of 450 bits, the maximum error for calculating the first case was of the order of magnitude of 1×10^{-130}. Finally, for the second case, it was assured that the stepsize (in increasing the solids volume fraction) did not influence the results. From a step number of 50 onwards, corresponding to a maximum stepsize of 1% in ϕ, the number did not have a significant effect on the results.

References

[1] D. Curvers, S.P. Usher, A.R. Kilcullen, P.J. Scales, H. Saveyn, P. Van der Meeren, The influence of ionic strength and osmotic pressure on the dewatering behaviour of sewage sludge, Chemical Engineering Science 64 (2009) 2448–2454.

[2] P.B. Sørensen, J.A. Hansen, Extreme solid compressibility in biological sludge dewatering, Water Science and Technology 28 (1993) 133–143.

[3] F. Tiller, W. Leu, Basic data fitting in filtration, Journal of the Chinese Institute of Chemical Engineers 11 (1980) 61–70.

[4] K. Keiding, M.R. Rasmussen, Osmotic effects in sludge dewatering, Advances in Environmental Research 7 (2003) 641–645.

[5] K. Keiding, L. Wybrandt, P. Nielsen, Remember the water – a comment on EPS colligative properties, Water Science and Technology 43 (6) (2001) 17–23.

[6] V. Legrand, D. Hourdet, R. Audebert, D. Snidaro, Deswelling and flocculation of gel networks: Application to sludge dewatering, Water Research 32 (12) (1998) 3662–3672.

[7] H. Liu, H.H.P. Fang, Extraction of extracellular polymeric substances (EPS) of sludges, Journal of Biotechnology 95 (2002) 249–256.

[8] Y. Liu, H.H.P. Fang, Influences of extracellular polymeric substances (EPS) on flocculation, settling and dewatering of activated sludge, Critical Reviews in Environmental Science and Technology 33 (2003) 237–273.

[9] B. Jin, B.M. Wilén, P. Lant, Impacts of morphological, physical and chemical properties of sludge flocs on dewaterability of activated sludge, Chemical Engineering Journal 98 (2004) 115–126.

[10] A Raszka, M. Chorvatova, J. Wanner, The role and significance of extracellular polymers in activated sludge. Part I: literature review, Acta Hydrochimica Et Hydrobiologica 34 (2006) 411–424.

[11] F. Jorand, F. Zartarian, F. Thomas, J. Block, J. Bottero, G. Villemin, V. Urbain, J. Manem, Chemical and structural (2D) linkage between bacteria within activated-sludge flocs, Water Research 29 (7) (1995) 1639–1647.

[12] D. Snidaro, F. Zartarian, F. Jorand, J.Y. Bottero, J.C. Block, J. Manem, Characterization of activated sludge flocs, Water Science & Technology 36 (1997) 313–320.

[13] D. Sanin, P.A. Vesilind, Bioflocculation of activated sludge: the role of calium ions and extracellular polymers, Environmental Technology 21 (2000) 1405–1412.

[14] R.M. Wu, D.J. Lee, T.D. Waite, J. Guan, Multilevel structure of sludge flocs, Journal of Colloid and Interface Science 252 (2002) 383–392.

[15] C.P. Chu, D.J. Lee, Multiscale structure of biological flocs, Chemical Engineering Science 59 (2004) 1875–1883.

[16] B.M. Wilén, M. Onuki, M. Hermansson, D. Lumley, T. Mino, Microbial community structure in activated sludge floc analysed by fluorescence in sity hybridisation and its relation to floc stability, Water Research 42 (2008) 2300–2308.

[17] M.L. Christensen, M. Hinge, The influence of creep on cake solid volume fraction during filtration of core–shell particles, Colloids and Surfaces A: Physicochemical and Engineering Aspects 320 (2008) 227–232.

[18] T. Seviour, M. Pijuan, T. Nicholson, J. Keller, Z. Yuan, Understanding the properties of aerobic sludge granules as hydrogels, Biotechnology and Bioengineering 102 (2008) 1483–1493.
[19] D. Jean, D.J. Lee, Effects of salinity on expression dewatering of activated sludge, Journal of Colloid and Interface Science 215 (1999) 443–445.
[20] P. Flory, Principles of Polymer Chemistry, 7th ed., Cornell University Press, London, 1969.
[21] R.A. Robinson, R.H. Stokes, Electrolyte Solutions, 2nd ed., Butterworths, Bath, 1968.
[22] A.R.G. Lang, Osmotic coefficients and water potentials of sodium chloride solutions from 0 to 40 degrees celsius, Australian Journal of Chemistry 20 (1967) 2017–2023.
[23] J. Miladinovic, R. Ninkovic, M. Todorovic, Osmotic and activity coefficients of $\{y\mathrm{KCl}+(1-y)\mathrm{MgCl_2}\}(\mathrm{aq})$ at $T=298.15$ K, Journal of Solution Chemistry 36 (11–12) (2007) 1401–1419.
[24] F. Horkay, I. Tasaki, P.J. Basser, Osmotic swelling of polyacrylate hydrogels in physiological salt solutions, Biomacromolecules 1 (2000) 84–90.
[25] A. Fernández-Nieves, A. Fernández-Barbero, B. Vincent, F.J. de las Nieves, Charge controlled swelling of microgel particles, Macromolecules 33 (2000) 2114–2118.
[26] W. Bowen, P. Williams, The osmotic pressure of electrostatically stabilized colloidal dispersions, Journal of Colloid and Interface Science 184 (1996) 214–250.
[27] M.F. Dignac, V. Urbain, D. Rybacki, A. Bruchet, D. Snidaro, P. Scribe, Chemical description of extracellular polymers: implication on activated sludge floc structure, Water Science & Technology 38 (1998) 45–53.
[28] A. Pohlmeier, S. Haber-Pohlmeier, Ionization of short polymethacrylic acid: titration, dls, and model calculations, Journal of Colloid and Interface Science 273 (2004) 369–380.
[29] D. Curvers, K.C. Maes, H. Saveyn, B. De Baets, S. Miller, P. Van der Meeren, Modelling the electro-osmotically enhanced pressure dewatering of activated sludge, Chemical Engineering Science 62 (2007) 2267–2276.
[30] L.H. Mikkelsen, Applications and limitations of the colloid titration method for measuring activated sludge surface charges, Water Research 37 (2003) 2458–2466.
[31] R. Buscall, L.R. White, The consolidation of concentrated suspensions. 1. The theory of sedimentation, Journal of the Chemical Society – Faraday Transactions I 83 (1987) 873–891.
[32] W. Stein et al., Sage Mathematics Software (Version 4.2.1), The Sage Development Team, 2009, http://www.sagemath.org.